Progress In Electromagnetics Research, PIER 10, 187–216, 1995

FINITE ELEMENT ANALYSIS OF OPTICAL WAVEGUIDES

B. M. A. Rahman

1. Introduction

The optimization of the performance of optical guided wave devices requires a knowledge of their propagation characteristics and field distributions, and their dependence on the fabrication parameters. As the range of guiding structures becomes more intricate, so the need for computer analysis becomes greater and thus more demanding. Therefore, there is a particular interest in theoretical methods of waveguide analysis which has attracted the attention of many researchers. It is

appropriate to refer to a general review paper on different numerical methods by Saad [1] and a review paper on the finite element method by Rahman, Fernandez and Davies [2] for further details.

Various types of analysis methods for optical waveguides have been proposed and used and some of these methods are described elsewhere in this book. Among the different numerical approaches, the finite element method has established itself as a powerful method throughout engineering for its flexibility and versatility, being used in complicated structural, thermal, fluid flow, semiconductor, and electromagnetic problems. This method is particularly advantageous for electromagnetic field problems, because of its applicability to waveguides with arbitrary shape, arbitrary refractive index profile, and anisotropic or nonlinear materials. The finite element method has been widely used during the last two decades in the analysis of various optical waveguide structures. Thus it is probably the waveguide analysis method that is the most generally applicable and most versatile.

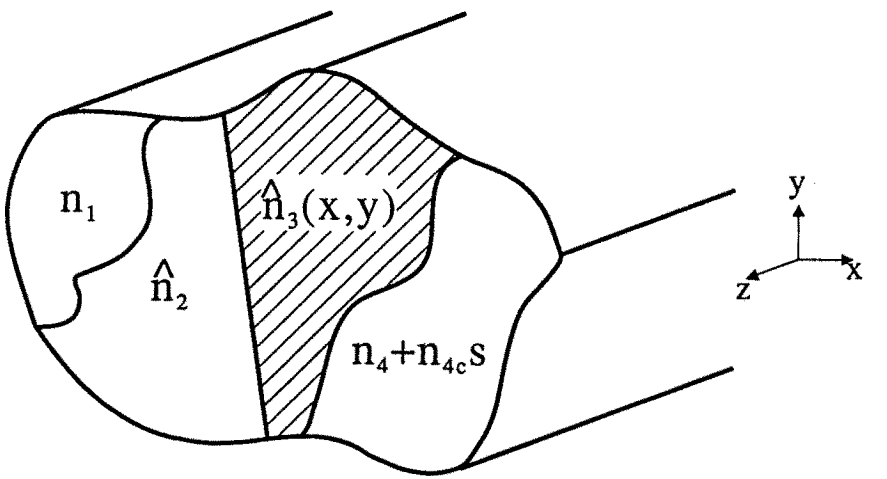

Figure 1. A general arbitrarily shaped optical waveguide geometry, which consists of several regions.

This chapter is concerned with the use of two-dimensional finite element techniques applied to optical waveguide problems. These may be understood by considering an arbitrarily shaped optical waveguide,

in Figure 1, which is composed of several different materials, each one of which can be described by arbitrary permittivity and permeability tensors ε and μ. The waveguide is assumed to be uniform along its longitudinal z axis. Assuming the time and z variation to be given by $\exp(j\omega t)$ and $\exp(-j\beta z)$ functions respectively, the electromagnetic fields at the angular frequency ω have the form:

$$\begin{aligned} \mathcal{H}(x,y,z,t) &= \mathbf{H}(x,y)\ \exp\ j(\omega t - \beta z) \\ \mathcal{E}(x,y,z,t) &= \mathbf{E}(x,y)\ \exp\ j(\omega t - \beta z) \end{aligned} \tag{1}$$

where β is the propagation constant in the positive z-direction. The general geometry of the guide can, if necessary, be quite complicated, with an arbitrary permittivity profile $\varepsilon(x,y)$ in the transverse $(x-y)$ directions.

2. Variational Formulations

Finite element formulations are usually established via a variational or a Galerkin (method of moments [3] or weighted residuals) approach. The latter is more flexible but when possible, it is advantageous to take a variational approach, especially when one global parameter (like the propagation constant) is the required answer. We will only refer to this form of derivation in this chapter.

2.1 Scalar Approximation

Several different variational formulations have been proposed for use with the finite element method. The simplest is the scalar formulations, which consider only one field component and these have been used for solving optical waveguide problems [4–11]. This formulation is valid only in situations where the fields can be described as predominantly TE or TM and one form suitable for quasi-TE modes can be written as [10]:

$$\mathbf{J}(\phi) = \int_{\Omega} \left[\left(\frac{\partial \phi}{\partial x} \right)^2 + \left(\frac{\partial \phi}{\partial y} \right)^2 + \left(\beta^2 - k_0^2\ n^2\ (x,y) \right)\ \phi^2 \right] dx\ dy \tag{2}$$

where β is the propagation constant, $n(x,y)$ is the refractive index profile and the integration is carried out over the waveguide cross-section domain Ω. A finite element program based on this formulation

yields β^2 as the eigenvalue of the matrix equation for a given free-space wave number, k_0 , and $\phi(x,y)$ is the transverse field distribution which is E_x for the quasi-TE modes. Similarly the scalar variational formulation for the quasi-TM modes can be written as [10]:

$$\mathbf{J}(\psi) = \int_{\Omega} \frac{1}{n^2(x,y)} \left[\left(\frac{\partial \psi}{\partial x} \right)^2 + \left(\frac{\partial \psi}{\partial y} \right)^2 + \left(\beta^2 - k_0^2 \, n^2(x,y) \right) \psi^2 \right] dx \, dy \tag{3}$$

In this formulation $\psi(x,y)$ is the transverse field distribution which is H_x for the quasi-TM modes.

In the finite element approximation [12–15], the primary dependent variables are replaced by a system of discretized variables over the domain of consideration. To achieve this, one first divides the entire waveguide cross section into a patchwork of subregions or elements, usually triangles or quadrilaterals. Elements can have various shapes, such as triangles or rectangles or even be with curved sides [16,17], and they can also be of various sizes. Triangles are commonly used because they are easy to adapt to complex shapes. Using many elements, any cross-section with a complex boundary and with arbitrary permittivity distribution can be accurately approximated. The simplest triangular element assumes a linear interpolation between the field values at the vertices of the triangle. Higher order interpolation polynomials are also used, with a larger number of nodal values (unknowns of the problem) in each element. By expressing the fields in terms of nodal values and with the assumed shape functions, the resulting field components are continuous over the whole domain.

To find these nodal fields, the usual (Rayleigh-Ritz) procedure is to force stationarity [12–15] of the functional with respect to each nodal variable. This yields a matrix eigenvalue equation, with vector $\mathbf{x}$ of nodal variables:

$$[\mathbf{A}]\{\mathbf{x}\} - \lambda[\mathbf{B}]\{\mathbf{x}\} = 0 \tag{4}$$

where $[\mathbf{A}]$ and $[\mathbf{B}]$ are real symmetric matrices, and $[\mathbf{B}]$ is also positive definite. The eigenvalue λ may be k_0^2 or β^2 depending on the

variational formulations. We emphasize that it is most desirable for the resulting matrix equation to be of this canonical form, to allow efficient and robust solution. This equation can be solved by one of various standard subroutines to obtain the different modal eigenvalues and associated eigenvectors.

2.2. Vector Formulations

The single scalar formulation is inadequate (except as an approximation) for the inherently hybrid mode situation of anisotropic or genuinely two dimensional, inhomogeneous optical waveguide problems. To represent accurately general waveguide fields, a vector formulation is necessary, with at least two field components. However, as we will see later, some vector formulations are affected by spurious or nonphysical solutions which appear mixed with the correct ones in the computation.

The finite element formulation in terms of the axial electric and magnetic field components, as the two-parameter basis for a variational formulation, has been used for analyzing various optical waveguides [10,17–24]. It has also been applied to anisotropic waveguides with a diagonal permittivity tensor [10,24].

This $E_z - H_z$ formulation cannot treat general anisotropic problems without destroying the canonical form of Eq. (4). Also, for a waveguide with an arbitrary dielectric distribution, enforcing boundary conditions in this method can be quite difficult. Another fundamental disadvantage for optical waveguide problems is that this $E_z - H_z$ formulation is based on axial field components which are the least important of the six components of the two vector **E** and **H** fields. Additionally, it is also affected by spurious solutions, and techniques to reduce them [10] can be at the expense of greatly increasing the computing cost.

In 1956, Berk [25] presented a number of vector variational formulations in the form of Rayleigh quotients for loss-free anisotropic waveguides and resonators in terms of the **H** field, the **E** field or a combination of both. Later, Morishita and Kumagai [26] and Chen and Lien [27] established general procedures to derive variational formulations for self-adjoint and non-self-adjoint operators.

A vector **E** formulation has been applied to analyze cylindrical waveguides [28], optical fibers [29,30], magnetically anisotropic waveguides [31] and 3-D cavities [32]. The **H**-field formulation has been ex-

tensively used for the solution of a variety of optical waveguide problems [4,33–43]. These formulations have attracted attention because they can be used to analyze general anisotropic but loss-less problems. The H-field formulation is more suited to dielectric waveguide problems where the magnetic field is continuous everywhere; furthermore, as the natural boundary condition [12–15] corresponds to that of an electric wall [36] boundary condition, one need not force the trial fields at conducting boundaries. This formulation can be written as [25,33]:

$$\omega^2 = \frac{\int (\nabla \times \mathbf{H})^* \cdot \hat{\varepsilon}^{-1} \cdot (\nabla \times \mathbf{H}) d\Omega}{\int \mathbf{H}^* \cdot \hat{\mu} \cdot \mathbf{H} \, d\Omega} \tag{5}$$

Integration is carried out over the waveguide cross-section Ω, where an asterisk denotes complex conjugation and $\hat{\varepsilon}$ and $\hat{\mu}$ are respectively the permittivity and permeability (which may be of arbitrary anisotropy) of the loss-free medium. Application of the Rayleigh-Ritz procedure to (5) leads to a similar eigenvalue problem as in (4), where now **A** is a complex Hermitian matrix (which can be reduced to the real symmetric case by using suitable transformation [35,39] for the loss-free condition), **B** is real symmetric and positive definite, and the eigenvectors **x** represent the unknown field components at the nodal points for different modes with ω^2 as their corresponding eigenvalues. Unfortunately, spurious solutions also appear in this formulation (as in the E-field formulation), although we will see later that these nonphysical modes can be avoided. In order to obtain a solution for a given wavelength, the β value has to be changed iteratively until the output eigenvalue corresponds to the correct wavelength.

Variational formulations, in terms of the transverse H-field or E-field components, have also been recently considered, including an implicit satisfaction of the divergence-free condition [44–49]. These formulations use the minimum number of variables required and can completely eliminate spurious solutions but at the expense of the complexity of the matrix problem or the sparsity of the matrices [45]. In this case, the matrix order can be reduced to two thirds of what is needed in the full vector formulation but more work will be needed in the future, particularly in the development of the formulations and in efficient matrix techniques [49] before these formulations become fully usable.

Othaka *et al.* [50] used a variational form and Williams and Cambrell [51] used the method of moments with the transverse component of **H**. Compared with the full vector **H**, this form can involve additional differentiation which is particularly disadvantageous with a finite element approach. Although there is recently a trend towards the employment of vector formulations based on only two components (of **E** or **H**) [47,49], a full vector form still has many advantages. This full vector formulation is quite easy to implement, most versatile with respect to the tensor ε, and leads to a standard matrix form for which robust and efficient solvers exist.

The full 6-component **E** and **H** formulation [52,53] does not appear to have much advantage over the **H**-field or **E**-field formulation, since in this case the degrees of freedom per node double. Apparent advantages reside in the simpler modeling of the basic equations, which allows the elimination of spurious modes, and it can be important when considering problems with special material properties.

2.3 Natural Boundary Conditions

The boundary condition which is automatically satisfied in the variational procedure is called the natural boundary condition [12–15]. The advantage of the variational formulation is that the natural boundary condition can be automatically satisfied if left free. The functional defined in equation (2) has the continuity $\frac{\partial \phi}{\partial \mathbf{n}}$ as the natural boundary condition, whereas the functional in equation (3) has the continuity $((\frac{1}{n^2})(\frac{\partial \psi}{\partial \mathbf{n}}))$ as the natural boundary condition where $\mathbf{n}$ is the outward unit normal vector. In contrast, the vector **H**-formulation given in equation (5) has the $\mathbf{n} \cdot \mathbf{H} = 0$ (Electric wall) as the natural boundary condition.

If necessary, we may also enforce the natural boundary condition to reduce the matrix order even these boundary conditions are satisfied automatically if left free. In some cases it may be necessary to change the unsuitable natural boundary condition by introducing additional surface integral around the desired boundary. If symmetry of a waveguide exists, then advantage of that should be taken by imposing that waveguide symmetry. However, it may be necessary to analyze the structure with complementary symmetry conditions to get all the modes but exploitation of the symmetry greatly reduces the computational cost.

3. The Finite Element Method

In the execution of the finite element method [12–15], the cross-section Ω of the optical waveguide concerned is first suitably divided into a number of subdomains or elements. Various types of elements are available for the finite element techniques. Elements are classified as one-, two-, and three-dimensional. The simplest example in one dimension would be a piecewise continuous linear function or, but for a more elaborate element it can be piecewise quadratic function. In two dimensions the elements are often triangles or rectangles. The most simple triangular element assumes a linear interpolation between the field values at the corner points (vertices) of the triangle. Within each of these element the trial function is approximated by a suitably chosen polynomial. In the simplest case the elements are triangular and first degree polynomials are used. By this procedure the transverse plane is covered with a grid of discrete nodes, which coincide with the corners of the triangles.

3.1 Shape Functions

The continuous field function $\phi(x, y)$ in the problem domain may be replaced by a set of discrete values $(\phi_p, p = 1, 2, 3, \ldots, m)$, where m is the total number of nodes. This function will be continuous across adjacent triangles, so that if the potential is interpreted like a third dimension, it can be viewed as a surface with many triangular facets. To be admissible functions, they must satisfy some conditions between the elements; usually the continuity of the field across the boundaries is preferred.

Inside each first order triangle and between the discrete nodes, ϕ is interpolated continuously. This can be achieved by introducing the nodal shape function $N_i(x, y)$. The field inside an element, $\phi_e(x, y)$, can be written as

$$\phi_e(x, y) = \sum_{i=1}^{3} N_i(x, y) \cdot \phi_i \tag{6}$$

where ϕ_i are the nodal field values. Equation (6) can be written in the matrix notation as,

$$\phi_e(x,y) = [N_1 \;\; N_2 \;\; N_3] \begin{Bmatrix} \phi_1 \\ \phi_2 \\ \phi_3 \end{Bmatrix} \tag{7}$$

$$= [N] \; \{\phi_e\} \tag{8}$$

where the row vector [N] is called the shape function matrix and the column vector $\{\phi_e\}$ is the vector corresponding to element nodal field values. The simplest first order triangular elements use a first-degree polynomial $(a + bx + cy)$ over each element. It can be shown that element shape function $\{\mathbf{N}\} \equiv [\mathbf{N}]^T$ can be written as

$$\{\mathbf{N}\} = \begin{bmatrix} N_1 \\ N_2 \\ N_3 \end{bmatrix} = \frac{1}{2Ae} \begin{bmatrix} x_2y_3 - x_3y_2 & y_2 - y_3 & x_3 - x_2 \\ x_3y_1 - x_1y_3 & y_3 - y_1 & x_1 - x_3 \\ x_1y_2 - x_2y_1 & y_1 - y_2 & x_2 - x_1 \end{bmatrix} \begin{bmatrix} 1 \\ x \\ y \end{bmatrix} \tag{9}$$

where T denotes a transpose, Ae the area of the triangle and x_1, x_2, x_3, y_1, y_2, and y_3 are respectively the x, y coordinates of the three nodes. $\{\mathbf{N}\}$ can also be written as

$$\{\mathbf{N}\} = \begin{bmatrix} N_1 \\ N_2 \\ N_3 \end{bmatrix} = \begin{bmatrix} a_1 & b_1x & c_1y \\ a_2 & b_2x & c_2y \\ a_3 & b_3x & c_3y \end{bmatrix} \tag{10}$$

By comparing equations (9) and (10) the coefficients a_i, b_i and c_i are calculated as

$$a_1 = \frac{x_2y_3 - x_3y_2}{2Ae}$$

$$b_1 = y_2 - y_3 \tag{11}$$

$$\text{and} \quad c_1 = x_3 - x_2$$

Similarly a_2, b_2, c_2, a_3, b_3, c_3 can be calculated by cyclic exchange of $1 \rightarrow 2 \rightarrow 3$ in equation 11.

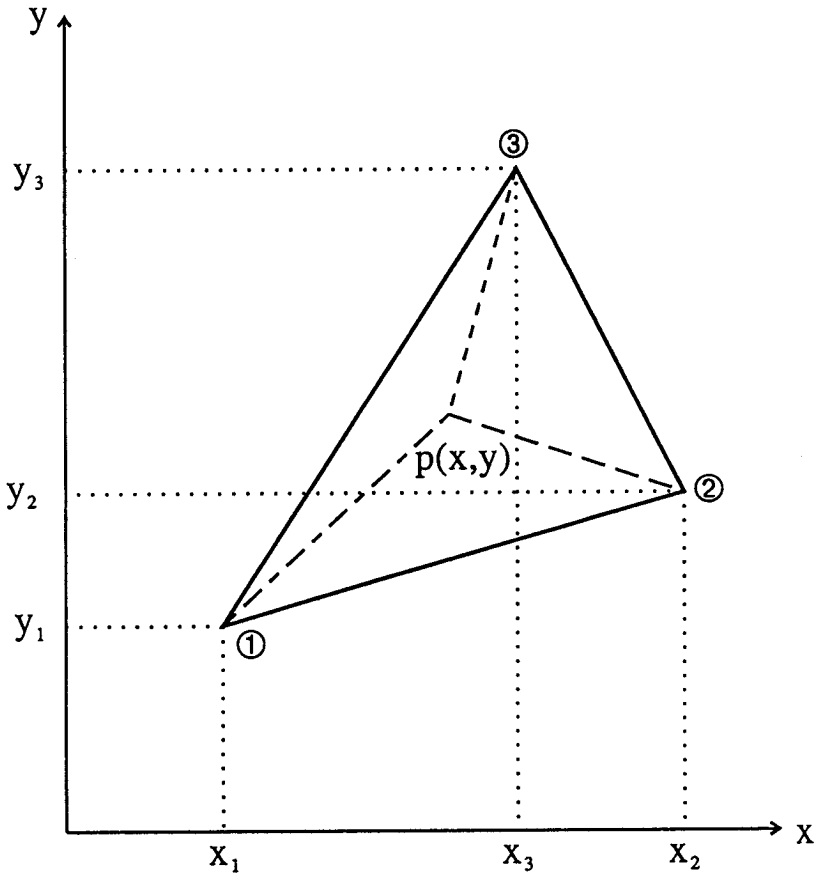

Figure 2. Coordinates and node numbers of a typical first order triangular element.

Consider the typical point P somewhere in the triangle of Fig. 2 with vertices 1, 2 and 3. N_1 can also be denoted by

$$N_1 = \frac{\text{area of the triangle P12}}{\text{area of the triangle 123}} \tag{12}$$

Similarly N_2 and N_3 can be defined and it immediately follows from

the area definition that

$$N_1 + N_2 + N_3 = 1 \tag{13}$$

3.2 Element and Global Matrices

For any one triangular element, the functional $\mathbf{J}^e$ can be calculated and the total functional $\mathbf{J}$ associated with the assemblage of many elements is, in general, the sum of all the n individual elements, where n is the total number of elements.

$$\mathbf{J} = \sum_{1}^{n} \mathbf{J}^e \tag{14}$$

$$= \left[\sum_{e=1}^{n} \int_{\Delta} \{\phi_e\}^T \left(\frac{\partial\{\mathbf{N}\}}{\partial x} \cdot \frac{\partial[\mathbf{N}]}{\partial x} + \frac{\partial\{\mathbf{N}\}}{\partial y} \cdot \frac{\partial[\mathbf{N}]}{\partial y} \right.\right.$$

$$\left.\left. + \beta^2 \{\mathbf{N}\}\,[\mathbf{N}] - k_0^2\, n_e\, \{\mathbf{N}\}\,[\mathbf{N}] \right) dx dy \right] \{\phi_e\} \tag{15}$$

The spatial derivative matrices $[X]$ and $[Y]$ can also be written in matrix form as

$$\frac{\partial[\mathbf{N}]}{\partial x} = \left[b_1 \;\; b_2 \;\; b_3 \right] = [X] \tag{16}$$

$$\frac{\partial[\mathbf{N}]}{\partial y} = \left[c_1 \;\; c_2 \;\; c_3 \right] = [Y] \tag{17}$$

where b_i and c_i are constant values only depend on the coordinate values of the three nodes for a given element which are given by the Eq. 11. The integration required in Eq. 16 can be easily carried out by using the following relation for a triangular element

$$\int_{\Delta} N_1^i \; N_2^j \; N_3^k \; d\Omega = \frac{i!\; j!\; k!\; 2!}{(i+j+k+2)!} \; Ae \tag{18}$$

After carrying out the integration, equation 16 can be written as

$$\mathbf{J} = \{\phi_p\}^T [\mathbf{A}] \{\phi_p\} - \lambda \; \{\phi_p\}^T [\mathbf{B}] \{\phi_p\} \tag{19}$$

where, the eigenvalue $\lambda = \beta^2$ and the [**A**] and [**B**] matrices, for the scalar formulation (2), are given by

$$\mathbf{A} = \sum_{1}^{n} \int_{\Delta} \left[\{X\}[X] + \{Y\}[Y] - k_0^2 \; n^2 \; \{N\}[N] \right] d\Omega \tag{20}$$

and

$$\mathbf{B} = \sum_{1}^{n} \int_{\Delta} \{N\}[N] \; d\Omega \tag{21}$$

where $\{X\}$ and $\{Y\}$ are the transposed column matrices of $[X]$ and $[Y]$ respectively. Since the energy expression of Eq.(20) is quadratic in nodal potentials, $\{\phi_p\}$, it must have a unique minimum with respect to each component of the potential vector $\{\phi_p\}$. To minimize the energy functional it is sufficient to set

$$\frac{\partial \mathbf{J}}{\partial \{\phi_p\}} = 0 \quad p = 1, 2, 3, ..., m \tag{22}$$

Following the minimization, we obtain the standard eigenvalue equation as shown in Eq. (3).

The vector formulation can be similarly derived except that instead of one unknown potential per node we have three unknown field potentials and they are H_x , H_y and H_z . Over each element, three components of the magnetic field can be written in the matrix form as

$$\left.\begin{aligned} H_x(x,y) &= [N]\{H_e^x\} \\ H_y(x,y) &= [N]\{H_e^y\} \\ H_z(x,y) &= [N]\{H_e^z\} \end{aligned}\right\} \tag{23}$$

where $\{H_e^x\}$, $\{H_e^y\}$, and $\{H_e^z\}$ are the three nodal field vectors of an element representing the $x, y,$ and z component of the magnetic field. The full vector magnetic field over an element can be written as

$$\{\mathbf{H_e}\} = \left\{\begin{matrix} \mathbf{x} & \{H_e^x\} \\ \mathbf{y} & \{H_e^y\} \\ \mathbf{z} & \{H_e^z\} \end{matrix}\right\} \tag{24}$$

Application of the standard finite element techniques to find stationary condition to the vector **H**-formulation given in equation (5) will yield the same generalized eigenvalue equation as shown in (4). But for this vector formulation, matrix **A** will be a complex Hermitian matrix and **B** will be a real symmetric positive definite matrix.

3.3 Matrix Solution Techniques

Solving waveguide problems by finite elements, the key factor affecting storage requirements and computational effort is the choice of algorithm to solve the matrix equation. In equation (4) the matrices **A** and **B** are highly sparse, the sparsity increasing with the order of the matrices and decreasing with the polynomial order of the shape functions [13]. The advantage of higher order basis functions for the fields is that it gives a more accurate solution for a given matrix order, but it involves an increased programming effort, particularly when considering anisotropic materials, infinite elements, and penalty functions. Another disadvantage of higher order polynomials (again for a given matrix order) is that it increases the density of the matrix. It must be emphasized here that the trade-off and the optimum choice between low- and high-order polynomials depends crucially on the matrix algorithm used. For instance, to take the extreme case of a fully dense matrix algorithm being used to solve equation (4), the optimum choice of polynomial order would be high - but of course this would be in the knowledge of the gross inefficiency of using a dense matrix algorithm. By contrast, at the other extreme one can use a matrix routine which considers only the nonzero elements of the upper or lower triangle of the symmetric real matrices. This has been used [54,33] with a specially developed arbitrary sparse matrix algorithm which solves the eigenvalue problem by an iteration process applied simultaneously to a subspace of eigenvectors; the method of subspace iteration [55]. This matrix solution technique does not need any initial guess for the field eigenvector, which is generated from random number generator to avoid any initial bias.

4. Numerical Results for Channel Waveguides

The finite element method has been applied to a wide variety of optical guided wave devices, for example, optical fibers [6, 18, 23, 40, 44, 56], slab waveguides [8], channel waveguides [8, 10, 33, 35, 37, 44], rib waveguides [5, 19, 38], directional couplers [17, 35, 44], electro-optic modulators [9,41], parametric oscillators [57], nonlinear optical waveguides [58–60], semiconductor amplifier [61] and semiconductor lasers [4]. In the spirit of this book we will show some examples of its application for channel waveguides.

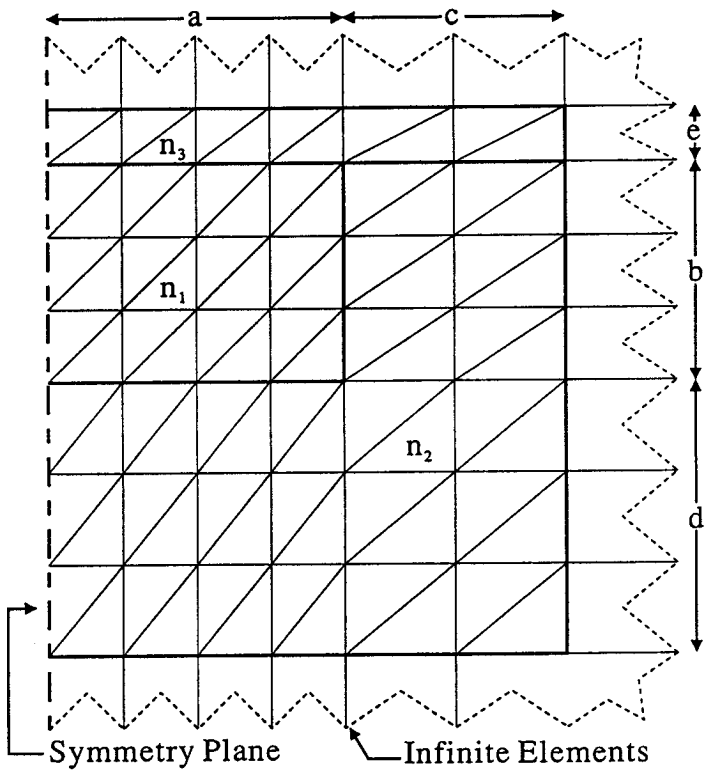

Figure 3. Discretization of a channel waveguide with orthodox and infinite elements.

4.1 Analysis of step index channel waveguide

In the finite element method, the cross-section of a waveguide is first subdivided into a patchwork of elements. It is quite laborious to input transverse coordinate data for all the nodes and element topology information. In general, a simple semi-automatic mesh generation program can provide all this information. As a first example we have considered a simple step index channel waveguide. A simple mesh with only 6 and 7 x-side and y-side mesh divisions respectively is shown in Fig. 3. For the available one-fold symmetry the grid covers only a part of the half plane with $x \geq 0$. It is composed of six domains, each of which consists of uniform rectangular grids. Half of the waveguide cross-section is represented by 84 first-order elements and some infinite element. All these elements can have different refractive indices but for a simple step index channel waveguide we need only three refractive index values.

Modes in channel waveguides are neither pure TE nor pure TM. In two-dimensional optical waveguides they are generally classified as the E^x_{mn} modes if the transverse electric field is primarily in the x-direction and E^y_{mn} modes if the transverse electric field is primarily in the y-direction. The m and n subscripts denote the number of maxima for the principal field component in the x and y directions, respectively. The E^x_{mn} can also be denoted as H^y_{mn} and similarly E^y_{mn} modes as H^x_{mn} modes. The lowest order mode has $m = 1$ and $n = 1$. For most purposes, the E^x_{mn} modes can be as considered quasi-TE modes while the E^y_{mn} modes can be considered as quasi-TM modes.

Figure 4 shows the variation of the normalized propagation constant, V,

$$V = \frac{(\frac{\beta}{k_0})^2 - n_2^2}{n_1^2 - n_2^2} \tag{25}$$

for the H^y_{11} and H^y_{21} modes (quasi TE modes) for the step index channel waveguide. In this example guide depth (b) and half-guide width (a) are varied and the core (n_1), substrate (n_2), and cladding (n_3) refractive indices are taken to be 2.30, 2.29, and 1.0 respectively. The wavelength is considered here as 0.850 μm. We have analyzed this waveguide structure using the vector H-formulation with 3200 first order elements. It takes less than 2 minutes to compute on a Sun Sparcstation 2. The dimensions c, d, and e should be such that orthodox boundary walls would not influence the solutions. To obtain

H^y_{mn} modes with m odd or even only, the symmetry wall along $y = 0$ should to be an electric wall or a magnetic wall respectively.

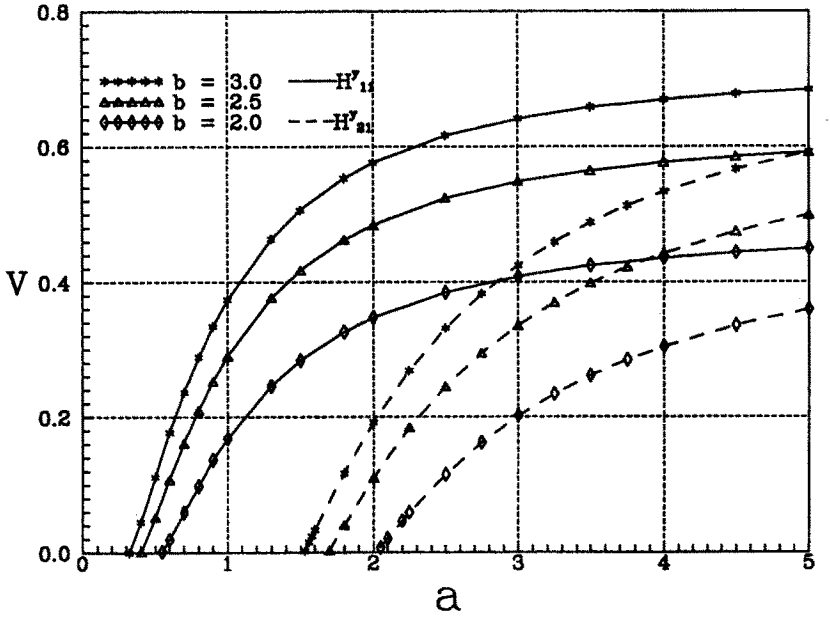

Figure 4. Dispersion characteristics for a step-channel waveguide.

4.2 Effect of Mesh Divisions

In the finite element method the solution accuracy improves [50] with the mesh refinement like the finite difference method. Figure 5 illustrates the effect of mesh divisions when $a = 3\,\mu$m and $b = 3\,\mu$m. This figure shows monotonic convergence with the mesh divisions. Note that in this figure the normalized propagation constant (which itself represents an expanded version of the propagation constant) is drawn in an enlarged scale to show the variation. It can be also noticed that the higher order mode converges slower than the fundamental mode as more mesh divisions are required to represent faster spatial field variations.

Convergence of the finite element solution is often studied by refining the size of the elements. Accuracy of results can be considerably increased by careful extrapolation techniques [16,38]. The technique is based on solving the physical problem with say two or three rather coarse meshes and extrapolating systematically from these results with considerable savings in computer time. If the pattern of element shapes is suitably preserved, then a powerful extrapolation procedure such as Aitken's extrapolation procedure [16,38] can be employed. In this technique mesh refinement should follow a fixed geometrical ratio and the results for the three calculations are put into the following extrapolation formulae [38]

$$X = X_{r+1} - \frac{(X_{r+1} - X_r)^2}{X_{r+1} - 2X_r + X_{r-1}} \tag{26}$$

Dotted lines in Fig. 5 are the extrapolated results using the Aitken's procedure.

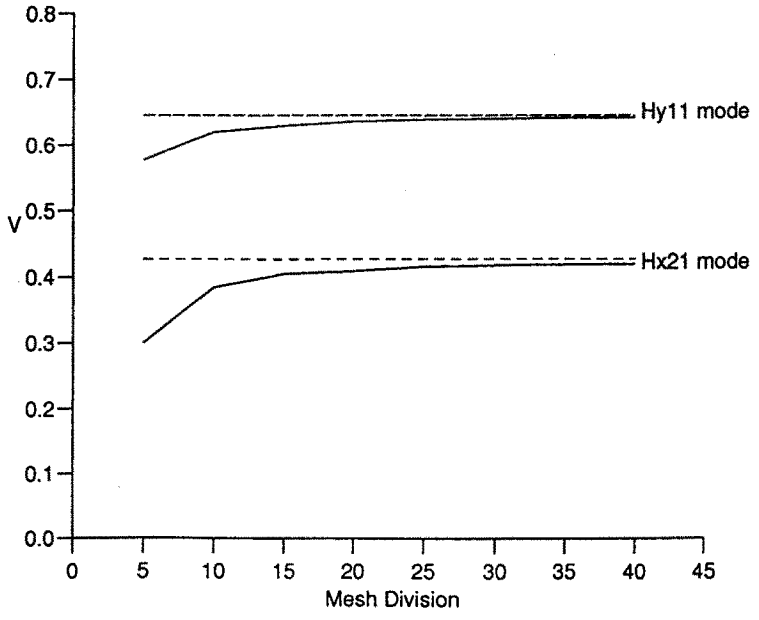

Figure 5. The convergence of the finite element solution with the mesh divisions.

It is convenient to have an automatic and interactive mesh generation program. More advanced packages can have sophisticated features, such as adaptive remeshing. Figure 6 shows such an adaptive mesh for a step channel waveguide. It can be observed that the center of the guide has a finer mesh compared to the much coarser mesh further away from the core. Using such adaptive remeshing [60–62] the accuracy of the solution can be improved for a given number of elements.

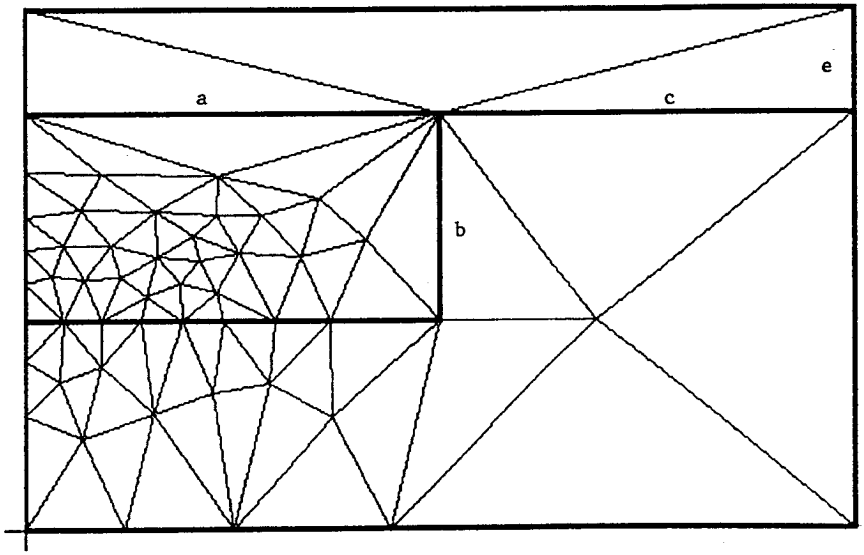

Figure 6. Adaptive meshes for the above channel waveguide using 92 first order elements.

4.3 Effect of Infinite Elements

Traditionally open-type optical waveguides are represented by restricting the problem domain up to a limit and filling the region with orthodox elements. However, this crude approach either introduces a significant error when the boundary is too close, or needs the consideration of an excessively large domain. One adaptive technique is to shift the virtual boundary wall recursively [22] to satisfy a criterion for maximum field strength at that wall. Open-boundary problems may be tackled more elegantly by introducing infinite elements. Adding these

infinite elements along the outer boundary of orthodox finite elements, any open-type optical waveguide cross-sectional domain can be represented very conveniently. These infinite elements extend the domain of explicit field representation to infinity without increasing the matrix order [33], so that the computational time is virtually unchanged.

In Cartesian coordinates, if an element is extended to infinity in the positive x direction, then we can consider the following shape function [33]

$$N(x,y) = N_y(y) \cdot N_x(x) = N_y(y) \cdot \exp[-x/L_x] \tag{27}$$

where L_x is the decay length in the x-direction. Similarly, elements can extend to the y-direction or in both directions.

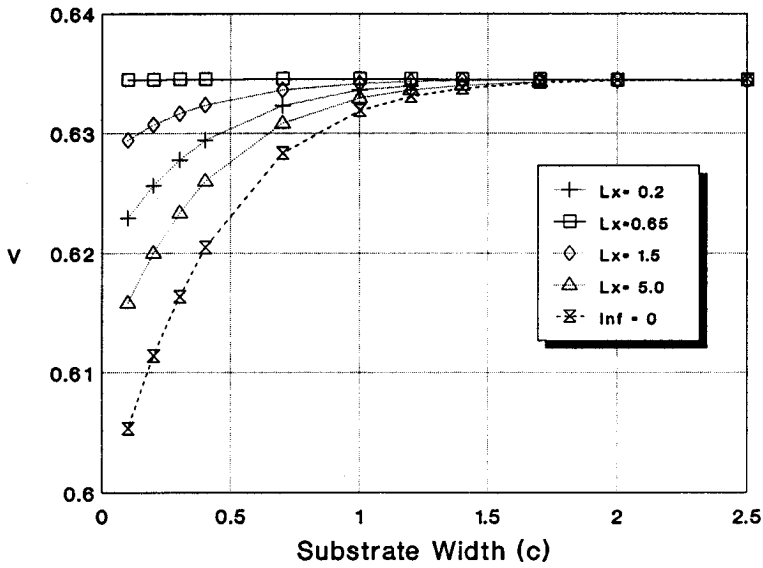

Figure 7. Effect of the artificial boundary wall position and the infinite elements at the same location.

A pending question in applying this technique is the selection of the free parameter, the decay length, which represents the decaying behavior of the field outside the core region. Although this free parameter can be optimized systematically [33, 38, 43, 63], in practice

almost any reasonable guess will be better than the default artificial boundary wall. Figure 7 illustrates the advantage of using infinite elements. The dashed line shows the effect of the fictitious right-side boundary wall position on the normalized propagation constant, when infinite elements are not used (Inf = 0). When infinite elements are used results improve considerably. Figure 7 also illustrates that when optimum decay value (in this example this was 0.65 μm) is used, the result is remarkably accurate even when the artificial wall (distance c) is only 0.1 μm from the guide core.

4.4 Effect of Penalty parameters

Perhaps the most serious difficulty in using some of the vector formulations is the appearance of extraneous nonphysical or spurious modes [2,64]. In the conventional vector finite element formulations, such as Eq. (5), the associated Euler equation is consistent with the two Maxwell curl equations but does not imply $\nabla \cdot B = 0$ which is believed to be responsible for the spurious modes. By imposing the divergence constraint by using the penalty technique, spurious solutions can be effectively removed. Besides removing them from the region of interest the penalty procedure also improves the eigenvector quality. A variational expression with the divergence-free constraint ($\nabla \cdot H = 0$) imposed in a least-square sense is given by [34,37]:

$$\omega^2 = \frac{\int (\nabla \times \mathbf{H})^* \cdot \hat{\varepsilon}^{-1} \cdot (\nabla \times \mathbf{H})\, d\Omega \;+\; \alpha \int (\nabla \cdot \mathbf{H})^* \cdot (\nabla \cdot \mathbf{H})\, d\Omega}{\int \mathbf{H}^* \cdot \hat{\mu} \cdot \mathbf{H}\, d\Omega} \tag{28}$$

It is necessary to comment on the free term α, the penalty coefficient, because the accuracy of the solution depends on its value. Generally, with the larger α value, the solutions get more stable but their accuracy deteriorates. On the other hand, the smaller the values of α becomes, the better the accuracy of the physical solutions tend to become. However, with the smaller α value, more spurious solutions appear and if a spurious solution couples with a physical solutions to form two degenerative eigenvectors, then the accuracy of the physical solution may be worse or very unpredictable. By considering eigenvalues λ_1 for $\alpha = \alpha_1$ and λ_2 for $\alpha = \alpha_2$ respectively, the correct eigenvalue $\lambda_0\,(\alpha = 0)$ can be extrapolated [40,56]. It is also observed from our experience that spurious solutions can be avoided by setting

$\alpha \cong 1/n_s^2$. This error is very small for reasonable mesh refinement. Figure 8 illustrates the effect of the penalty parameter for the H_{11}^y mode.

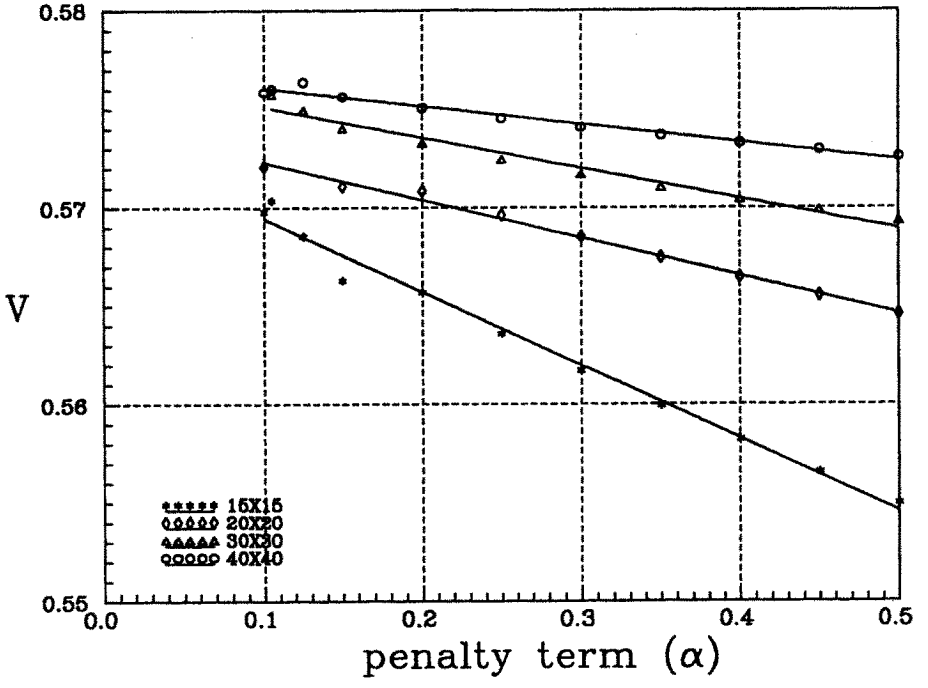

Figure 8. Variation of the effective indices with the penalty value.

One of the advantages of using the penalty method is that it does not increase the matrix order and the additional computational time is negligible [34]. Another big advantage of using penalty term is that eigenvector quality is vastly improved [34]. Figure 9(a) shows an eigenvector with $\alpha = 0.2$, in contrast to the eigenvector at $\alpha = 0.0$, that is no penalty term is used, is shown in Figure 9(b).

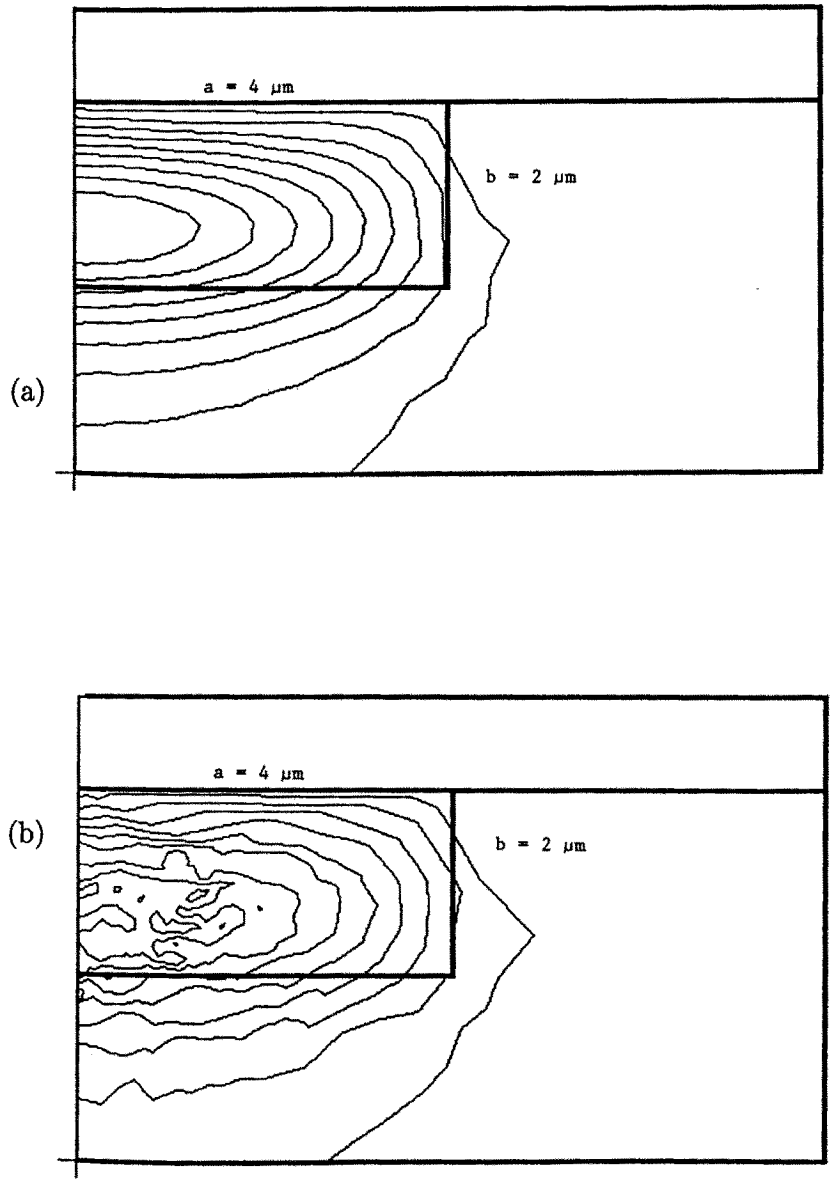

Figure 9. Constant normalized H_y field contours in 10% increments for the H_{11}^y mode with (a) $\alpha = 0.20$ and (b) $\alpha = 0$.

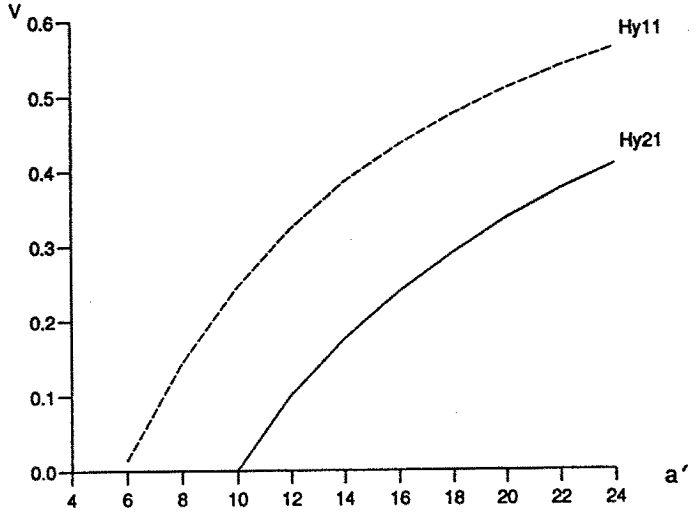

Figure 10. Dispersion characteristics for a diffused channel waveguide.

4.5 Diffused Channel Waveguide

The channel waveguides formed by diffusion are of considerable interest because of their applications to integrated optical devices. Due to several important physical properties of the crystal materials, such as large electro-optical, elasto-optical and second order nonlinearities, a number of interesting devices such as switches and modulators [9,41] and parametric oscillators [57] can be realized. Optical channel waveguides can be formed in $LiNbO_3$ by the in-diffusion of thin titanium stripes. The diffusion induced refractive index variation can be described by [11]:

$$n(x,y) = n_s(x,y) + \Delta n \cdot f(x) \cdot g(y) \tag{29}$$

The finite element method can clearly represent a waveguide with any given arbitrary index profile as each element can have different refractive indices. We can assign each element with different refractive index values following any given $f(x)$ and $g(y)$ refractive index profile, such as of the Gaussian, exponential or error function type. Figure 10 shows the variation of the normalized propagation constant for the

diffused channel waveguide with normalized dimension of the guide a', where

$$a' = k_0 \; a\sqrt{(n_s + \Delta n)^2 - n_s^2} \tag{30}$$

and a, the width of the titanium strip, was 6.0 μm. In this example n_s and Δn were 2.0 and 0.1 and both $f(x)$ and $f(y)$ were Gaussian types with diffusion length 3.0 μm.

5. Concluding Remarks

Unfortunately most of the optical waveguides do not lend themselves well to analytical techniques. In this book it has been demonstrated that numerical analysis becomes standard for most of the dielectric waveguide forms which are usable at optical frequencies. Finite element methods have undoubtedly become a powerful tool for the analysis of electromagnetic problems and they stand as some of the most important techniques for carrying out such numerical analysis for such optical waveguides. With this method, the propagation characteristics of a wide range of practical optical waveguides are easily attainable. Besides the characterization of optical waveguides, there have been numerous applications for various guided wave devices, such as directional couplers, electro-optic modulators, parametric oscillators, semiconductor lasers and amplifiers.

Several ways to formulate this method using variational approaches have been discussed in reference [2]. The full vector **H**-field formulation still appears to be the most convenient for a wide range of practical optical waveguides. Although it uses three rather than the minimum of two components to describe the fields, the resultant matrix problem can be solved using standard software library packages. Its main drawback, the existence of spurious modes, can be partially cured using a penalty method. This formulation is fundamentally more accurate than scalar forms since it can represent true hybrid modes.

In this chapter we have presented results for simple step-index and diffused channel waveguides using vector **H**-formulation. We have also discussed the effect of two free parameters, the penalty term (α) and the decay constant and their selection criteria.

Recent advances in computer technology have brought a rapid change in the form of traditional finite element analysis. Furthermore, the mathematics required in defining the element verges on the trivial,

and computer programming at the very simple level can produce many useful results. The advent of fast processing and computer graphics has allowed the incorporation of pre- and post-processing facilities to such an extent that nowadays it is hard to conceive of a finite element program without some of these. The enormous increase of available memory in the present modest workstations with fast processors has caused a trend towards even more complicated modeling, allowing the solution of problems that only a few years ago were too big even for the largest machines. Undoubtedly this trend will mean that in the near future, more and more electromagnetic field problems will be solved routinely using these numerical techniques. In particular, as the computer becomes faster, more powerful and cheaper, CAD based on finite element method will be seen to have generated wider interest.

Acknowledgment

The author would like to acknowledge the long standing collaboration with Professor J. Brian Davies' group at University College, London. Thanks also to all the students in the research group but particularly to T. Wongcharoen and F. A. Katsriku. Finally acknowledgment to Professor K. T. V. Grattan for his encouragement and support.

References

1. Saad, S. M., "Review of numerical methods for the analysis of arbitrarily-shaped microwave and optical dielectric waveguides," *IEEE Trans. Microwave Theory Tech.*, Vol. MTT-33, 894–899, Oct. 1985.
2. Rahman, B. M. A., F. A. Fernandez, and J. B. Davies, "Review of finite element methods for microwave and optical waveguides," *P. IEEE*, Vol. 79, 1442–1448, 1991.
3. Harrington, R. F., *Field Computation by Moment Methods*, R. E. Krieger Publishing Company, Florida, 1968.
4. Hayata, K., M. Koshiba, and M. Suzuki, "Lateral mode analysis of buried heterostructure diode lasers by the finite-element method," *IEEE J. Quantum Electron.*, Vol. QE-22, 781–788, June 1986.
5. Koshiba, M., K. Hayata, and M. Suzuki, "Approximate scalar finite-element analysis of anisotropic optical waveguides with

off-diagonal elements in a permittivity tensor," *IEEE Trans. Microwave Theory Tech.*, Vol. MTT-32, 587–593, June 1984.
6. Chiang, K. S., "Finite-element analysis of optical fibres with iterative treatment of the infinite 2-D space," *Opt. Quantum Electron.*, Vol. 17, No. 6, 381–391, 1985.
7. Wu, R. B., and C. H. Chen, "A scalar variational conformal mapping technique for weakly guiding dielectric waveguides," *IEEE J. Quantum Electron.*, Vol. QE-22, 603–609, May 1986.
8. Koshiba, M., K. Hayata, and M. Suzuki, "Approximate scalar finite-element analysis of anisotropic optical waveguides," *Electron. Lett.*, Vol. 18, 411–413, May 1982.
9. Mustacich, R.V., "Scalar finite element analysis of electro-optic modulation in diffused channel waveguides and poled waveguides in polymer thin films," *Appl. Opt.*, Vol. 27, 3732–3737, Sept. 1988.
10. Mabaya, N., P. E. Lagasse, and P. Vandenbulcke, "Finite element analysis of optical waveguides," *IEEE Trans. Microwave Theory Tech.*, Vol. MTT-29, 600–605, June 1981.
11. Strake, E., G. P. Bava, and I. Montrosset, "Guided modes of Ti:LiNbO3 channel waveguides: A novel quasi-analytical technique in comparison with the scalar finite-element method," *J. Lightwave Technol*, Vol. LT-6, 1126–1135, 1988.
12. Zienkiewicz, O. C., *The Finite Element Method*, 3rd. ed. London, England: McGraw-Hill, 1977.
13. Silvester, P. P., and R. L. Ferrari, *Finite Elements for Electrical Engineers*, 2nd. ed., Cambridge Press, 1990.
14. Davies, J. B., "The finite element method," in T. Itoh ed., *Numerical Techniques for Microwave and Millimeter-wave Passive Structures*, 33–132, Wiley 1989.
15. Reddy, J. N., *An Introduction to the Finite Element Method*, McGraw Hill, New York, 1984.
16. Daly, P., "Finite element approach to propagation in elliptical and parabolic waveguides," *Int. J. Num. Meth. Eng.*, Vol. 20, 681–688, 1984.
17. Welt, D., and J. Webb, "Finite-element analysis of dielectric waveguides with curved boundaries," *IEEE Trans. Microwave Theory Tech.*, Vol. MTT-33, 576–585, July 1985.
18. Yeh, C., S. B. Dong, and W. Oliver, "Arbitrarily shaped inhomogeneous optical fiber or integrated optical waveguides," *J. Appl. Phys.*, Vol. 46, 2125–2129, May 1975.

19. Bird, T. S., "Propagation and radiation characteristics of rib waveguide," *Electron. Lett.*, Vol. 13, 401–403, July 1977.
20. Okamoto, K., and T. Okoshi, "Vectorial wave analysis of inhomogeneous optical fibres using finite element method," *IEEE Trans. Microwave Theory Tech.*, Vol. MTT-26, 109–114, 1978.
21. Yeh, C., K. Ha, S. B. Dong, and W. P. Brown, "Single-mode optical waveguides," *Appl. Opt.*, Vol. 18, 1490–1504, May 1979.
22. Ikeuchi, M., H. Sawami, and H. Niki, "Analysis of open-type dielectric waveguides by the finite-element iterative method," *IEEE Trans. Microwave Theory Tech.*, Vol. MTT-29, 234–239, Mar. 1981.
23. Oyamada, K., and T. Okoshi, "Two-dimensional finite-element calculation of propagation characteristics of axially nonsymmetrical optical fibres," *Radio Sci.*, Vol. 17, 109–116, Jan.-Feb. 1982.
24. Vandenbulcke, P., and P. E. Lagasse, "Eigenmode analysis of anisotropic optical fibres or integrated optical waveguides," *Electron. Lett.*, Vol. 12, 120–122, Mar. 1976.
25. Berk, A. D., "Variational principles for electromagnetic resonators and waveguides," *IRE Trans. Antennas Propagat.*, Vol. AP-4, 104–111, Apr. 1956.
26. Morishita, K., and N. Kumagai, "Unified approach to the derivation of variational expression for electromagnetic fields," *IEEE Trans. Microwave Theory Tech.*, Vol. MTT-25, 34–40, Jan. 1977.
27. Chen, C. H., and C. Lien, "The variational principle for nonself-adjoint electromagnetic problems," *IEEE Trans. Microwave Theory Tech.*, Vol. MTT-28, 878–886, Aug. 1980.
28. English, W. J., and F. J. Young, "An E vector variational formulation of the Maxwell equations for cylindrical waveguide problems," *IEEE Trans. Microwave Theory Tech.*, Vol. MTT-19, 40–46, Jan. 1971.
29. Katz, J., "Novel solution of 2-D waveguides using the finite element method," *Appl. Opt.*, Vol. 21, 2747–2750, Aug. 1982.
30. Koshiba, M., K. Hayata, and M. Suzuki, "Vector E-field finite-element analysis of dielectric optical waveguides," *Applied Optics*, Vol. 25, 10–11, 1986.
31. Koshiba, M., K. Hayata, and M. Suzuki, "Finite-element formulation in terms of the electric-field vector for electromagnetic waveguide problems," *IEEE Trans. Microwave Theory Tech.*, Vol. MTT-33, 900–905, Oct. 1985.

32. Hara, M., T. Wada, T. Fukasawa, and F. Kikuchi, "A three dimensional analysis of RF electromagnetic fields by the finite element method," *IEEE Trans. Magnetics*, Vol. MAG-19, 2417–2420, Nov. 1983.
33. Rahman, B. M. A., and J. B. Davies, "Finite-element analysis of optical and microwave waveguide problems," *IEEE Trans. Microwave Theory Tech.*, Vol. MTT-32, 20–28, Jan. 1984.
34. Rahman, B. M. A., and J. B. Davies, "Penalty function improvement of waveguide solution by finite elements," *IEEE Trans. Microwave Theory Tech.*, Vol. MTT-32, 922–928, Aug. 1984.
35. Rahman, B. M. A., and J. B. Davies, "Finite-element solution of integrated optical waveguides," *J. Lightwave Technol.*, Vol. LT-2, 682–688, Oct. 1984.
36. Konrad, A., "Vector variational formulation of electromagnetic fields in anisotropic media," *IEEE Trans. Microwave Theory Tech.*, Vol. MTT-24, 553–559, Sept. 1976.
37. Koshiba, M., K. Hayata, and M. Suzuki, "Improved finite-element formulation in terms of the magnetic field vector for dielectric waveguides," *IEEE Trans. Microwave Theory Tech.*, Vol. MTT-33, 227–233, Mar. 1985.
38. Rahman, B. M. A., and J. B. Davies, "Vector-H finite element solution of GaAs/GaAlAs rib waveguides," *IEE Proc. Pt.J, Optoelectron.*, Vol. 132, 349–353, Dec. 1985.
39. Koshiba, M., K. Hayata, and M. Suzuki, "Finite-element solution of anisotropic waveguides with arbitrary tensor permittivity," *J. Lightwave Technol.*, Vol. LT-4, 121–126, Feb. 1986.
40. Hayata, K., M. Eguchi, M. Koshiba, and M. Suzuki, "Vectorial wave analysis of side-tunnel type polarization-maintaining optical fibers by variational finite elements," *J. Lightwave Technol.*, Vol. LT-4, 1090–1096, Aug. 1986.
41. Young, T. P., "Design of integrated optical circuits using finite elements," *IEE Proc. Pt.A* , Vol. 135, 135–144, Mar. 1988.
42. Kobelansky, A. J., and J. P. Webb, "Eliminating spurious modes in finite-element waveguide problems by using divergence-free fields," *Electron. Lett.* Vol. 22, 569–570, May 1986.
43. McDougall, M. J., and J. P. Webb, "Infinite elements for the analysis of open dielectric waveguides," *IEEE Trans. Microwave Theory Tech.*, Vol. MTT-37, 1724–1731, Nov. 1989.

44. Su, C.-C., "A combined method for dielectric waveguides using the finite-element technique and the surface integral equations method," *IEEE Trans. Microwave Theory Tech.*, Vol. MTT-34, 1140–1146, Nov. 1986.
45. Hayata, K., M. Koshiba, M. Eguchi, and M. Suzuki, "Vectorial finite-element method without any spurious solutions for dielectric waveguiding problems using transverse magnetic-field component," *IEEE Trans. Microwave Theory Tech.*, Vol. MTT-34, 1120–1124, Nov. 1986.
46. Hayata, K., K. Miura, and M. Koshiba, "Finite-element formulation for lossy waveguides," *IEEE Trans. Microwave Theory Tech.*, Vol. MTT-36, 268–276, Feb. 1988.
47. Chew, W. C., and M. A. Nasir, "A variational analysis of anisotropic, inhomogeneous dielectric waveguides," *IEEE Trans. Microwave Theory Tech.*, Vol. MTT-37, 661–668, Apr. 1989.
48. Cvetkovic, S. R., F. A. Fernandez, and J. B. Davies, "Finite element analysis of wave propagation in lossy inhomogeneous anisotropic dielectric media based on variational principles," *in 1988 IEEE AP-S Int. Antenna Propagat. Symp. Dig.*, Syracuse, New York, June 1988, 1130–1133.
49. Fernandez, F.A., and Y. Lu, "Variational finite element analysis of dielectric waveguides with no spurious solutions," *Electron. Lett.*, Vol. 26, 2125–2126, Dec. 1990.
50. Ohtaka, M., M. Matsuhara, and N. Kumagai, "Analysis of the guided modes in slab-coupled waveguides using a variational method," *IEEE J. Quantum Electron.*, Vol. QE-12, 378–382, July 1976.
51. Williams, C. G., and G. K. Cambrell, "Numerical solution of surface waveguide modes using transverse field components," *IEEE Trans. Microwave Theory Tech.*, Vol. MTT-22, 329–330, Mar. 1974.
52. English, W.J., "Vector variational solutions of inhomogeneously loaded cylindrical waveguide structures," *IEEE Trans. Microwave Theory Tech.*, Vol. 19, 9–18, Jan. 1971.
53. Svedin, J. A. M., "A numerically efficient finite-element formulation for the general waveguide problem without spurious modes," *IEEE Trans. Microwave Theory Tech.*, Vol. MTT-37, 1708–1715, Nov. 1989.

54. Davies, J. B., F. A. Fernandez, and G. Y. Philippou, "Finite element analysis of all modes in cavities with circular symmetry," *IEEE Trans. Microwave Theory Tech.*, Vol. MTT-30, 1975–1980, Nov. 1982.
55. Bathe, K. J., and E. L. Wilson, *Numerical Methods in Finite Element Analysis.* Englewood Cliffs. NJ: Prentice Hall, 1976.
56. Hayata, K., M. Koshiba, and M. Suzuki, "Vectorial wave analysis of stress - applied polarization - maintaining optical fibers by the finite-element method," *J. Lightwave Technol.*, Vol. LT-4, 133–139, 1986.
57. Bava, G. P., I. Montrosset, W. Sohler, and H. Suche, "Numerical modeling of Ti:LiNbO3 integrated optical parametric oscillators," *IEEE J. Quantum Electron*, Vol. 23, 42–51, 1987.
58. Rahman, B. M. A., and J. B. Davies, "Finite element solution of nonlinear bistable optical waveguides," *Int. J. Optoelectronics.*, Vol. 4, 153–161, Mar. 1989.
59. Hayata, K., and M. Koshiba, "Full vectorial analysis of nonlinear-optical waveguides," *J. Opt. Soc. Am. B*, Vol. 5, 2494–2501, Dec. 1988.
60. Ettinger, R. D., F. A. Fernandez, B. M. A. Rahman, and J. B. Davies, "Vector finite element solution of saturable nonlinear strip-loaded optical waveguides," *IEEE Photonic Technology Letters*, Vol. 2, 147–149, 1991.
61. Young, T. P., "Finite element modeling of a polarization independent optical amplifier," *J. Lightwave Technol*, Vol. 10, 626–632, 1992.
62. Lee, J-F., D-K. Sun, and Z. J. Cendes, "Full-wave analysis of dielectric waveguides using tangential vector finite elements," *IEEE Trans. Microwave Theory Tech.*, Vol. MTT-39, 1262–1271, 1991
63. Hayata, K., M. Eguchi, and M. Koshiba, "Self-consistent finite-/infinite element scheme for unbounded guided wave problems," *IEEE Trans. Microwave Theory Tech.*, Vol. MTT-36, 614–616, Mar. 1988.
64. Koshiba, M., K. Hayata, and M. Suzuki, "Finite-element method analysis of microwave and optical waveguides - Trends in countermeasures to spurious solutions," *Electron. and Comm. in Japan*, Pt. 2, Vol. 70, 96–108, 1987.